

Mechanical Performance and Weight Reduction of Additively Manufactured Ti-6Al-4V Bolts Aimed for Supply Chain Resiliency of Critical Material

Henrik Neibig^a, Salil Bapat^b, and Ajay P. Malshe^{b,*}

^a School of Mechanical Engineering, Purdue University, West Lafayette, IN 47907, USA
GEARE Exchange student from Germany (Karlsruhe Institute of Technology)

^b Manufacturing and Materials Research Laboratories (MMRL), School of Mechanical
Engineering, Purdue University, West Lafayette, IN 47906, USA

* Corresponding author: amalshe@purdue.edu

Abstract

This study investigates the feasibility of replacing conventionally manufactured aerospace bolts with topology-optimized Ti-6Al-4V bolts produced via Laser Powder Bed Fusion (LPBF), as a case study for enhancing supply chain resiliency. A solid baseline and three weight-reduced variants (2.5%, 5%, 10%) featuring internal gyroid lattices were fabricated and tensile tested per NASM1312-8. Mass reduction and dimensional accuracy were evaluated using precision scales and X-ray computed tomography (X-ray CT). Performance was compared to machined Ti-6Al-4V bar stock bolts. While the optimized designs retained near-comparable tensile strength among LPBF variants, they showed significant reductions relative to bar stock. The results highlight the need for careful process control and deeper engineering insight when substituting traditional parts with additively manufactured alternatives for resiliency in manufacturing.

1 Introduction and Background

Threaded fasteners are indispensable components in aerospace structures, providing critical load transfer and assembly integrity. Despite their relatively small size, they contribute significantly to overall system weight, particularly when manufactured from dense materials such as steel and nickel alloys. Titanium alloys, especially Ti-6Al-4V (Ti64), offer a compelling alternative due to their high strength-to-weight ratio, corrosion resistance, and temperature tolerance. However, conventional manufacturing of titanium fasteners is limited by machining complexity, high material cost, and restrictions on producing internal features or customized geometries for potential weight savings. In parallel, industry interest in supply chain decentralization has accelerated interest in producing certified parts closer to the point of use.

Additive manufacturing (AM), and specifically Laser Powder Bed Fusion (LPBF), offers new design freedoms for aerospace components. It enables the fabrication of complex internal structures, such as gyroid-based lattices, and supports mass customization and decentralized production. These capabilities make AM a promising candidate for producing weight-optimized fasteners on demand. Prior work has shown that lattice structures can reduce mass while maintaining global stiffness and strength, but few studies have addressed their performance in

fully threaded aerospace-grade bolts [1]. While promising, an important consideration toward adapting LPBF for flight-critical fasteners lies in demonstrating compliance with aerospace mechanical standards. AM parts often exhibit process-induced defects, anisotropic microstructures, and surface irregularities, all of which can degrade mechanical performance [2][3][4].

Additionally, Ti64 alloy is a critical raw material for many industrial applications, including biomedical and aerospace parts, and many of the target components for these applications require precision manufacturing and combinations of multiple manufacturing operations/equipment use due to complex design(s). Any disruption in the supply of Ti-alloy raw material can significantly impact the manufacturing and, in turn, lead to undesirable market consequences and thus serves as a motivation for this feasibility study.

The ability to manufacture complex and customized designs also makes AM an attractive candidate to deliver on-demand, on-site part production for increased resiliency, which is the focus of this research investigation. This study investigates the mechanical viability of Ti64 bolts manufactured by LPBF with varying levels of internal lattice-based designs to simulate limited access to available raw materials in the event of supply chain disruptions. The designs are evaluated against a machined baseline using tensile testing per NASM1312-8. Key focus areas include the influence of lattice topology on strength retention, manufacturing precision assessed through X-ray computed tomography (XCT), and failure behavior under axial loading.

2 Literature Review and Research Motivation

The adoption of AM in aerospace continues to grow, particularly for components where design complexity and weight are critical constraints. While laser powder bed fusion (LPBF) has already proven effective in fabricating components such as turbine blades and combustor parts, its potential for customized designs to meet resiliency metrics is relatively unexplored. As a part of this work, the authors focus on high-performance, load-bearing fasteners [5] as a case study where the customization of design could potentially benefit the on-demand and on-site manufacturing operations, as a part of the value proposition for AM, and also to manage potential supply chain disruptions. Unlike bulk structures, fasteners are subject to stringent geometric, surface, and mechanical requirements, especially when used in flight-critical assemblies. This study builds upon current knowledge by introducing functional, weight-reduced bolts with internal lattices and subjecting them to aerospace-relevant testing (NASM1312- 8). The outcomes of this feasibility work would potentially benefit future research in meeting these stringent requirements and challenges associated with the qualification of AM parts.

Current literature predominantly focuses on simplified tensile specimens, lattice coupons, or non-functional geometries when studying LPBF performance [6][7]. Although these studies establish fundamental relationships between process parameters, defect evolution, and lattice behavior, they do not sufficiently address how these findings translate to fully threaded components under aerospace qualification standards. Recent work exploring gyroid lattices in titanium alloys highlights their promise for isotropic strength and efficient energy distribution, yet functional integration within bolt geometries remains a significant gap [8]. AM with stress-based lattice designs could open up the design envelope to maximize the number of available resources,

which could be an important consideration for improving the resiliency of the production operations without compromising the performance.

In particular, this work aims to address the following research query: Does AM allow for resilient manufacturing operations in the wake of disruptions (simulated by reducing the material usage)? By exploring the trade-offs between mass reduction and mechanical reliability, this work aims to address whether additive manufacturing is a resilient process for manufacturing components of critical materials such as Ti64. It is hypothesized that topology-optimized Ti64 bolts, incorporating internal lattice-based weight reduction at levels of 2.5%, 5%, and 10%, will demonstrate comparable mechanical performance to each other and to the solid 0% weight-reduction baseline variant. Furthermore, these additively manufactured bolts are expected to exhibit tensile strength roughly comparable to that of conventionally manufactured bolts, while satisfying the geometric and mechanical requirements outlined in NASM1312-8 and relevant ASTM standards for aerospace fasteners. The specific details of the experimental approach are discussed below.

3 Experimental Details

To simulate limited access to the raw material as a stress test for resiliency, M8 bolt designs were modified with lattice geometry to progressively reduce the material usage. All bolt geometries conformed to the aerospace specifications for $M8 \times 1.25 \text{ mm} \times 30 \text{ mm}$ fasteners. LPBF was used to manufacture the test specimen. In addition to lattice-modified designs, fully solid test specimens (no designed porosity) were also additively manufactured. Additionally, M8 fasteners were also manufactured with a traditional machining approach for reference comparison. A total of 7 specimens were printed (machined) for each case. Further details of design methodology, manufacturing setup, and testing protocols are discussed below.

3.1 Design methodology

The study included additively manufactured samples with a solid bolt variant (S0, with no internal lattice porosity) and three weight-reduced variants with 2.5% (S2.5), 5% (S5), and 10% (S10) internal lattice-based volume reductions, as well as the machined reference variant (SM). Lattice placement followed a stress-based approach using von Mises equivalent stress derived from simulated loading, as shown in Figure 1. The lattice structure density and wall thickness changed with the simulated stress. The different variants were created by increasing a scalar factor in the stress field. Cross sections of the final designs are shown in Figure 2.

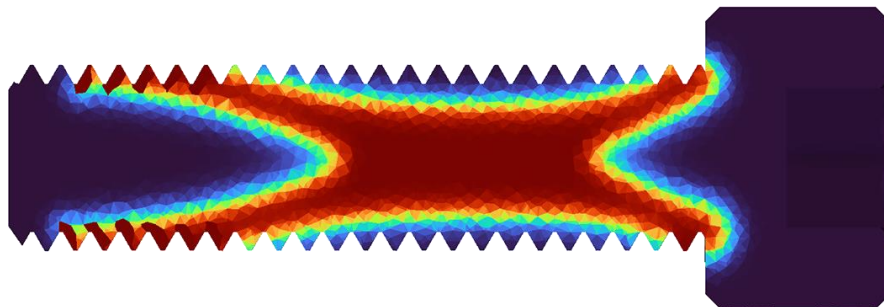


Figure 1: FEM simulation of von Mises stress distribution.

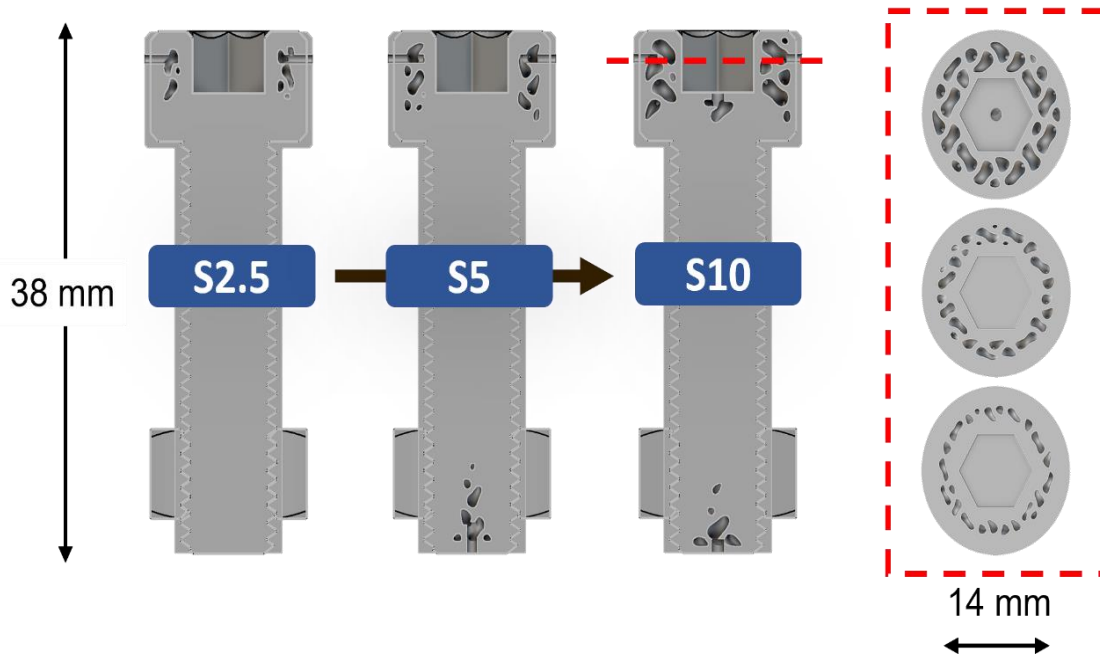


Figure 2: Vertical and top-head cross-sectional designs of bolt variants showing internal cavities for weight reduction (S2.5, S5, S10 samples).

3.2 Materials and manufacturing

The bolts were manufactured using Ti64 Grade 5 powder (ASTM Grade 5) with a particle size range of 15 μm to 45 μm . The chemical composition of the powder was approximately 80–90% titanium, 6–6.5% aluminum, and 3.8–4.5% vanadium. All bolts were assembled and tested using high-strength hex nuts conforming to DIN 934, with M8 \times 1.25 mm threads, a width of 13 mm, a height of 6.5 mm, and made from ISO Class 12 steel.

The material selection and dimensions were chosen to reflect standards commonly used in aerospace applications, ensuring the study’s relevance to real-world practices. Ti64 Grade 5 is a widely adopted alloy for structural components due to its favorable strength-to-weight ratio and well-documented performance. The M8 \times 1.25 mm bolt dimensions were selected because they represent a common industrial fastener size that is both compatible with additive manufacturing constraints and large enough to integrate internal lattice structures for meaningful weight reduction.

The bolts were produced via laser powder bed fusion (LPBF) using Matsuura Lumex Avance 25 equipment. The build orientation was vertical, with the bolt head placed flat on the build plate to avoid the need for support structures and minimize distortions. For this feasibility study, the potential influence of the build orientation on the strength was not considered as it was beyond the scope of the intended focus. The sintering process was executed with the following parameters based on previous tests to optimize print quality- laser power of 230 W, a laser spot diameter of 300 μm , scan speed of 800 mm/s, layer height of 50 μm , and hatch spacing of 130 μm . The hatch pattern was rotated by 67° on each successive layer to ensure structural homogeneity. No thermal treatment of the printed bolts was performed. Threads were machined as a post-processing

operation using light passes to reduce cutting forces during post-processing on a Haas ST20 CNC lathe by clamping the bolt head in a collet chuck. For the reference SM, a set of bolts was also machined from 15.875 mm round Ti64 rod stock.

3.3 Testing setup and protocols

Tensile testing was carried out according to NASM1312-8 using an Instron 34TM-50 machine at a constant strain rate of 1 mm min^{-1} , corresponding to approximately $35,000 \text{ N min}^{-1}$. Strain was recorded from crosshead displacement. The tests were conducted at $18 \text{ }^\circ\text{C}$. It should be noted that this is not a sufficient verification for a flight-ready part but rather a fundamental starting point for subsequent tests and an in-depth research study.

Mass measurements were taken before and after machining using an A&D Newton EJ-200 precision scale with 0.01 g resolution and a 210 g capacity. X-ray CT scans were performed at a voxel size of $15 \text{ }\mu\text{m}$, using a tube voltage of 190 kV and current of $180 \text{ }\mu\text{A}$, with 2100 projections. Fracture surfaces were analyzed post-failure using light microscopy at various magnifications. Table 1 summarizes the details of testing and characterization, as well as the rationale behind these measurements for interpretation and analysis.

Table 1: Summary of testing and measurements used in this research

Measurement	Details	Purpose
Weight measurement	A&D Newton EJ-200 precision scale with 0.01 g resolution and a 210 g capacity	Analyze and quantify the reduction in material usage.
X-ray CT scanning	Voxel size of $15 \text{ }\mu\text{m}$, using a tube voltage of 190 kV and current of $180 \text{ }\mu\text{A}$, with 2100 projections	3-D structural analysis and porosity maps.
Tensile testing	Instron 34TM-50, Strain rate – 1 mm/min , per NASM1312-8 standard	Study and compare the mechanical properties of the additively manufactured test specimens.
Fracture surface analysis	Optical microscope at various magnifications	Correlate the results on X-ray CT and tensile testing for process mechanism and interpretations.

4 Results and Discussion

4.1 Manufacturing observations

The manufacturing process produced generally consistent results across all weight-reduction variants. Slight bending was observed in several specimens, likely due to residual stress and thermal gradients during the LPBF process. The surface finish, while rough as

expected from as-printed titanium, was consistent across samples and did not present significant irregularities. Post-processing machining introduced some variability due to inconsistent clamping based on the rough and small surface of the head in the collet chuck. A slight taper was detected in the threads, likely resulting from deflection during machining. This led to variations in weight reduction after machining. Fatigue-related machining damage was observed post-test, with most AM bolts showing signs of cyclic bending fracture in the head radius, which could also indicate a reduced strength for most of the AM bolt specimens.

For the machined reference bolts (SM), all seven met dimensional requirements, and six were tested to failure. In the S0 group, two specimens failed during machining, and five were successfully tested. The S2.5 group had one machining failure and one specimen with thread defects, while the remaining five sample specimens were tensile tested. All seven specimens in the S5 and S10 groups were successfully printed and machined, with six tested in each case.

4.2 Weight reduction

The weight reduction was calculated by measuring bolt weights of each variant using a precision scale to compare the weight-reduced bolts to the average weight of the solid bolts. Figure 3 shows the measured weights for each porosity variant before and after post-process machining to realize threads. Table 2 summarizes the actual weight reduction before and after the machining process. The machining process induced higher variance in the weight reduction, but consistently increased the relative weight reduction as expected. The measured weight reduction was significantly less than the intended targets for each design. This discrepancy is primarily attributed to residual powder trapped within the lattice structures, which was verified using X-ray CT measurements discussed below. While the CAD model allowed for a theoretically near-complete removal of powder, in practice, surface imperfections and partially closed channels hindered effective powder evacuation, even with vibration and compressed air.

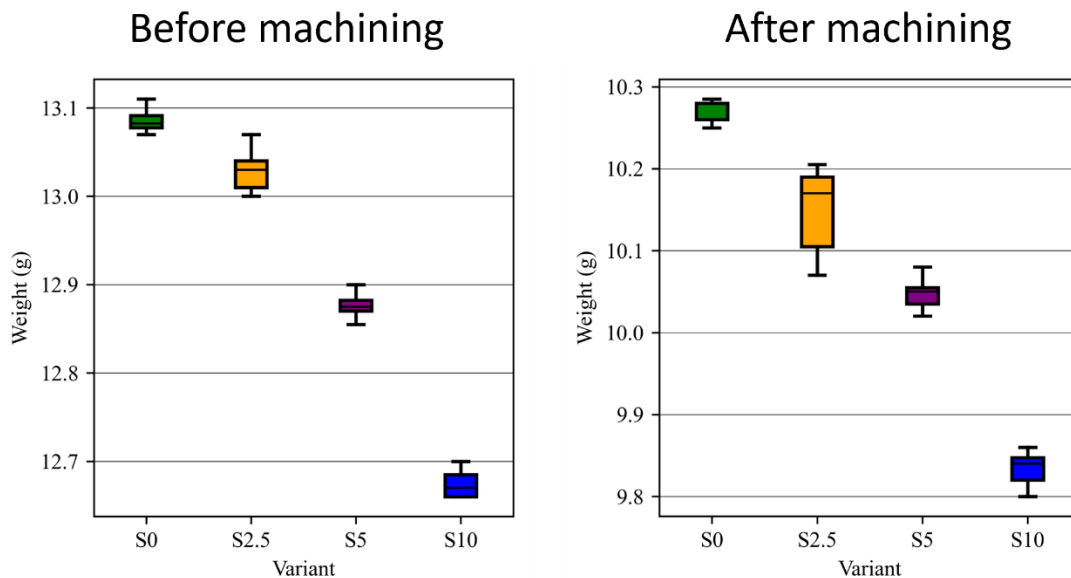


Figure 3: Average values of weights measured for each AM variant before and after post-processing machining operation for manufacturing threads.

Table 2: Achieved weight reduction relative to the solid baseline

Goal (%)	Before Machining (%)	After Machining (%)
0.0	0.000	0.000
2.5	0.441	1.359
5.0	1.603	2.180
10.0	3.192	4.259

4.3 X-ray CT analysis

Representative AM samples were characterized with X-ray CT scanning measurements to assess the geometric accuracy of the different bolt variants and verify alignment with the digital models. Due to time and cost considerations, one sample for each AM variant was chosen for these measurements. Figure 4 shows the scan results for all AM variants. Overall, the scans show good dimensional fidelity and slight wall thickness variations. The scans also reveal trapped unsintered powder within the lattice, which could not be removed post-processing. As discussed in section 4.2, while this residual powder affects the effective weight reduction, its mechanical influence is assumed to be negligible.

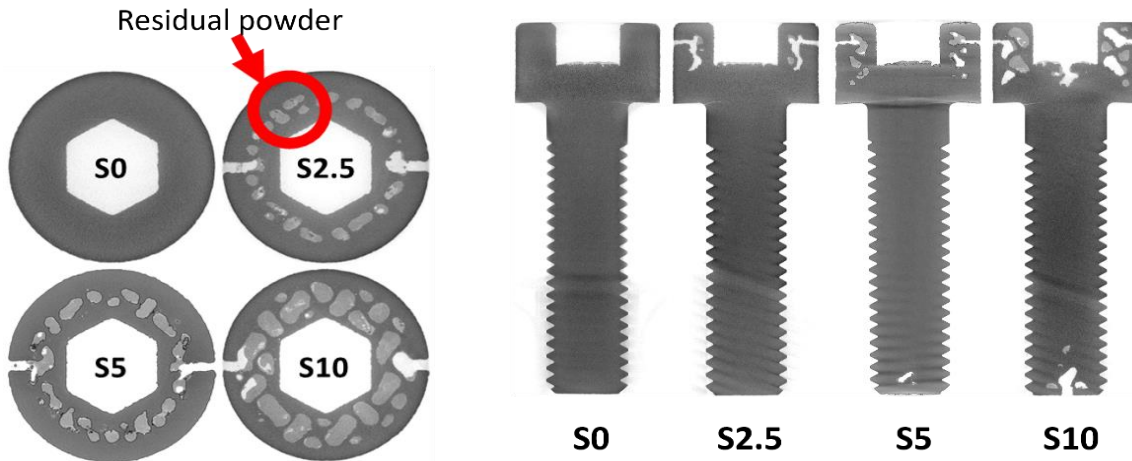


Figure 4: Top and cross-sectional X-ray CT images of representative bolts showing remnant residual powder inside designed cavities.

The X-ray CT scan also helped in identifying the crack in the head radius of the samples. The crack was not visible during visual inspection of the samples post-machining. The cracks in all 4 tested samples had matching size and location, shown as the pink colored volume visible in Figure 5. The authors believe that this is the manifestation of the bolts being clamped in the head region while machining the thread, which caused excessive stress at the neck region, resulting in a crack. Another important measure for the quality of a 3D print using the LPBF process is the porosity of the part, which should be 0% of the volume under ideal conditions and print settings. Pores over the size of 40 μm are big enough to be detected with the CT scan and can also be seen in Figure 5, with color varying with pore size. Table 3 quantifies the porosity by the volumetric percentage, which is consistently below 0.1% verifying that the chosen printing parameters were within the appropriate processing window.

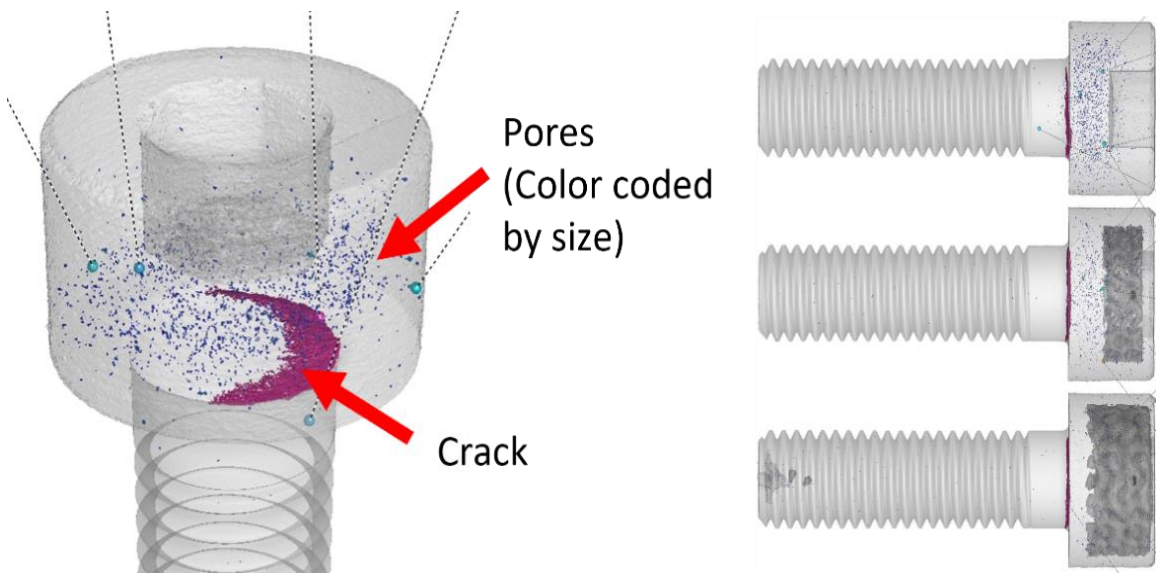


Figure 5: X-ray CT analysis revealing a crack at the bolt head observed in all AM samples.

Table 3: Volumetric porosity measurements from XCT analysis

Variant	Solid (mm ³)	Void (mm ³)	Porosity (%)
S0	2303.58	1.11	0.04817
S2.5	2223.00	1.02	0.04582
S5	2185.08	0.48	0.02198
S10	2093.05	1.07	0.05113

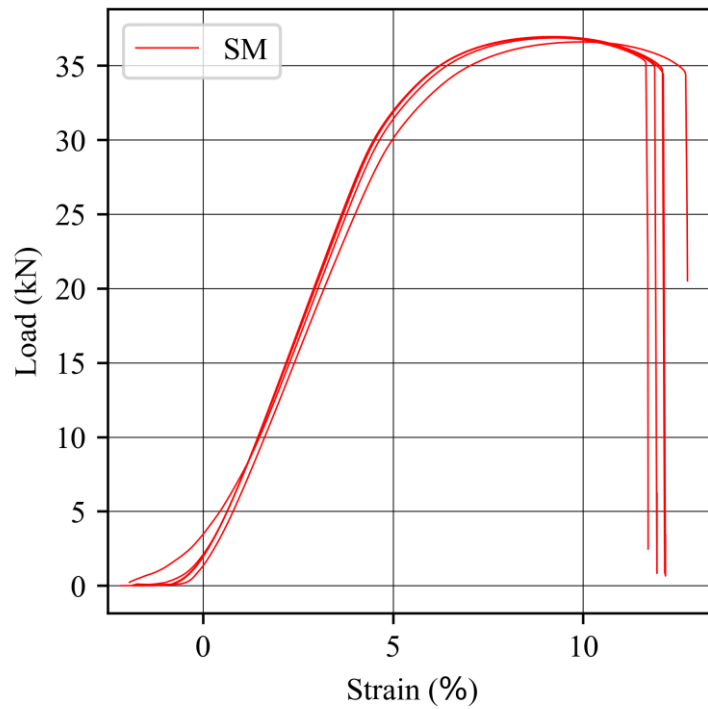


Figure 6: Tensile load-strain curves for reference machined bolts (SM).

4.4 Tensile testing results

The tensile behavior of conventionally manufactured titanium bolts exhibited classical ductile characteristics, as demonstrated by the load-strain curves in Figure 6. These specimens achieved consistent ultimate tensile strengths of about 36.8 kN with elongation exceeding 10%. Fractographic analysis (discussed in the next section) revealed fully dimpled rupture surfaces characteristic of micro-void coalescence, with finer striations observed near thread roots indicating localized plastic strain concentration. The absence of cleavage facets or intergranular features confirms the material's inherent ductility under quasi-static loading conditions.

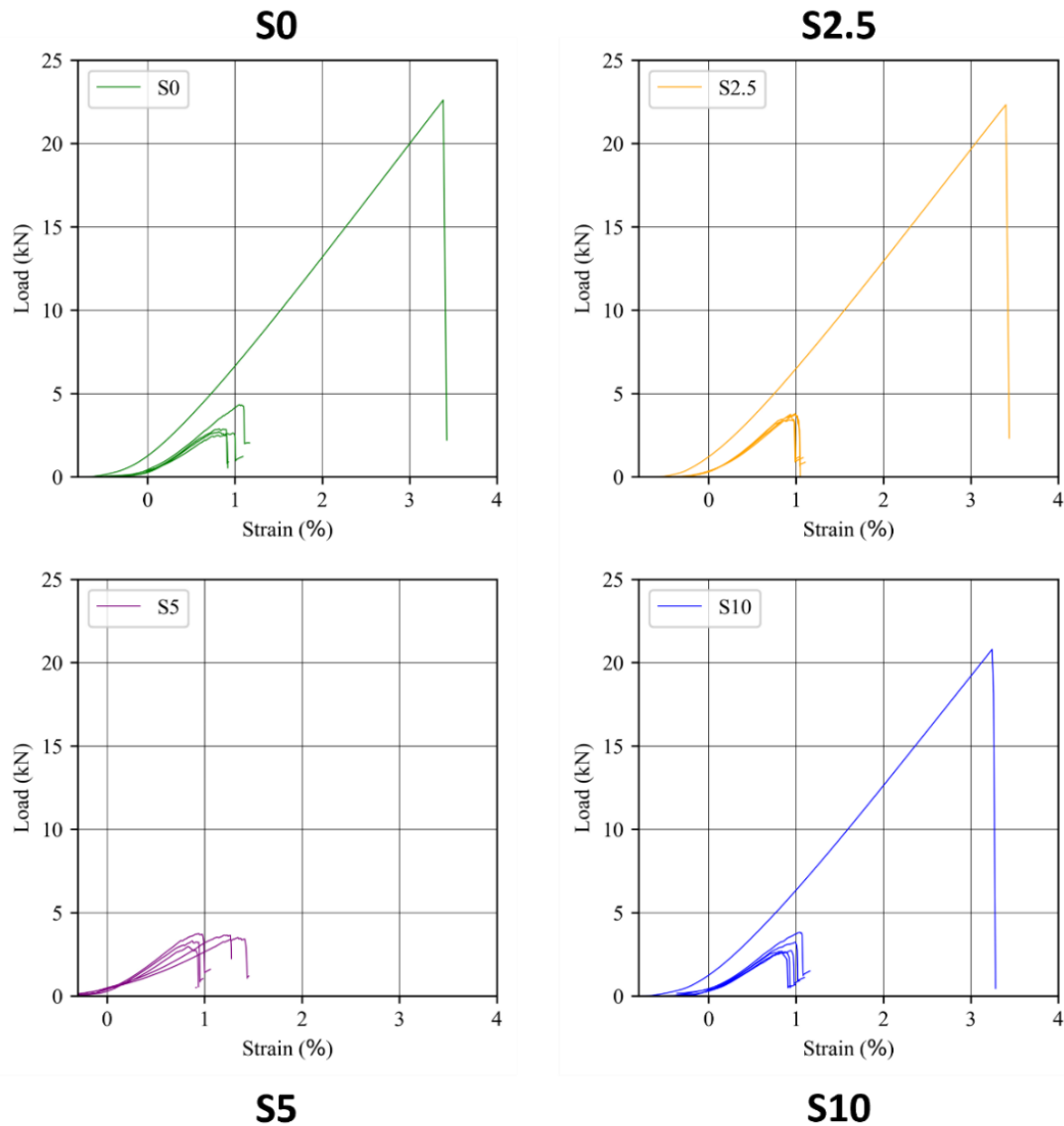


Figure 7: Tensile test data for all variants of AM bolts.

In contrast, additively manufactured sample specimens displayed markedly different mechanical responses and premature failures, as shown in Figure 7. This was attributed to the large machining-induced crack observed in the head region of bolts (Figure 5). The most severe

mechanical degradation occurred in these specimens, resulting in catastrophic failure around just 3.5 kN load - a 90% strength reduction compared to conventional counterparts. These pre-cracked specimens exhibited multiple sequential fractures, producing a distinctive stair-step load-displacement curve. The fracture surfaces transitioned from flat, featureless zones at crack initiation sites to propagation marks, demonstrating how stress intensification at defect sites combined with LPBF-induced microstructural heterogeneity likely resulted in the failure. As seen in Figure 7, all the samples for the S5 variant showed premature failure and are thus not included in the comparative analysis presented below.

Figure 8a shows the comparative plot of tensile test data for the best case for each sample variant. The LPBF-produced bolts demonstrated a 40.5% reduction in ultimate load (21.9 kN) and substantially limited ductility (3% strain-to-failure), also with all fractures initiating in the threaded region. Figure 8b shows zoomed-in comparative plots for all AM samples. As seen in the figure, the best-case AM sample specimens (assumed to be the samples that did not have machining-induced cracking in the head region) fractured abruptly within the linear elastic portion of the stress-strain curve, indicating a brittle failure mode. The fracture surfaces appeared significantly rougher than those of comparable components made from stock material. This increased roughness is attributed to the LPBF process characteristics, including columnar grain morphology, potential α' martensite formation, and distributed subsurface porosity, which collectively reduce the material's capacity for plastic deformation. The different variants exhibited similar performance, with the 10% weight-reduced specimen showing a decreased ultimate load, possibly attributable to the weight reduction, although the decrease is small enough for any conclusive interpretation in light of sample to sample variability in the AM parts and since only one sample from each set did not show premature failure due to machining-induced cracks limiting statistical analysis and repeatability testing.

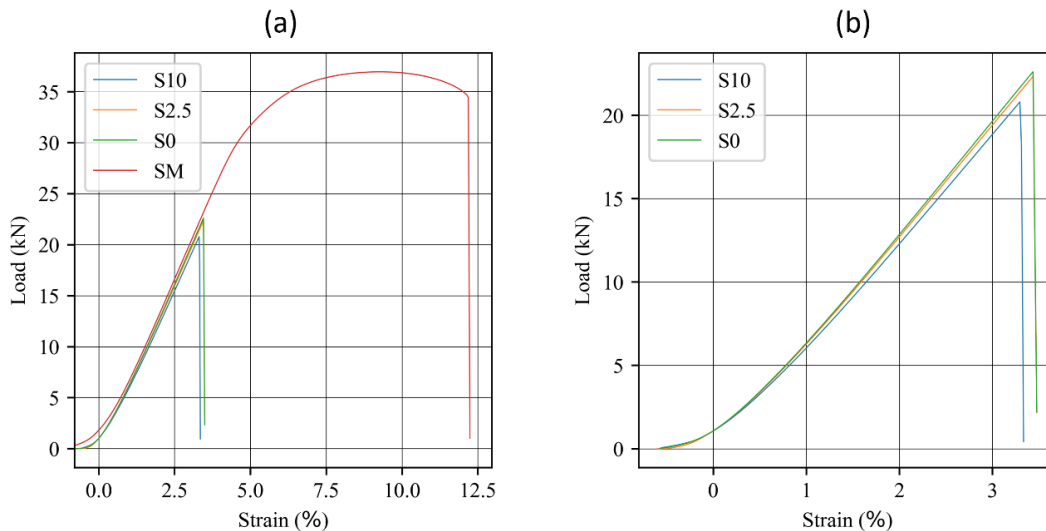


Figure 8: Tensile test comparison (a) best case tensile plots for AM bolt variants against machined (SM) bolt; (b) zoomed-in view of best case tensile plot for AM bolts.

Figure 9 shows the comparative summary of maximum loads for all manufactured samples, highlighting the critical importance of defect control in additively manufactured components. S10 showed marginally lower strength, though this preliminary observation requires verification through extended statistical analysis to account for manufacturing

variability. These results collectively demonstrate that while LPBF can produce functional titanium fasteners under simulated limited access to raw material, their mechanical performance remains highly sensitive to both inherent process-induced defects and post-processing and warrants further detailed investigation.

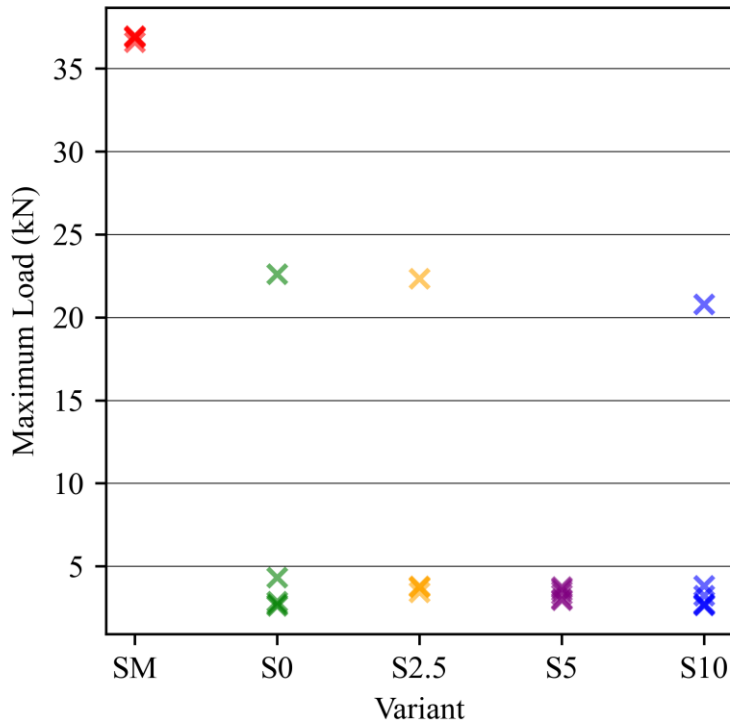


Figure 9: Peak tensile loads of all tested specimens.

4.5 Fracture surface analysis

As discussed in the above section, the majority of the AM-manufactured bolts resulted in premature failure due to machining-induced cracks, limiting a detailed comparison and analysis of AM parts against traditionally manufactured bolts. Due to this reason, a detailed fracture surface characterization was not performed, as only a handful of samples were available for meaningful comparison between different variants. However, preliminary fracture images still revealed some interesting trends as briefly discussed below.

Mainly, the samples with the best-case tensile plots (Figure 8a) all fractured in the threaded region. This also aligns with the observation that the samples that showed premature failure had a machining-induced crack in the head region. Figure 10 shows optical images of the fracture surface for the reference machined sample (SM). Figure 10 a-b show uniform rough surface features and little indication of porosity. Figure 10c shows the ruptured thread with ductile, elongated fracture. On the other hand, fractured surfaces for the representative AM sample (S2.5) shown in Figure 11a-b have remarkably different surface features. The surface has multiple jagged edges and sharp features, and at the same time, much more non-uniform roughness, indicating potential for the effect of AM-induced porosity. Similar to Figure 10c, a fractured thread is visible in Figure 11c. As opposed to the SM sample, this fractured thread has a sharp,

clean cut indicative of a catastrophic failure before plastic deformation, consistent with the observed tensile behavior. Other AM bolt variant samples also showed similar behavior.

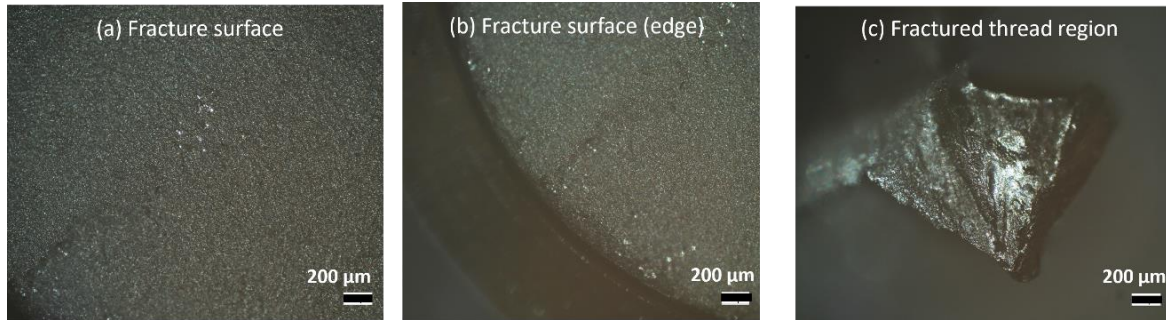


Figure 10: Optical micrographs of the fracture surface for reference machined (SM) samples: (a) and (b) fracture surface; (c) location of fracture in the threaded region. Fracture occurred in the threaded region.

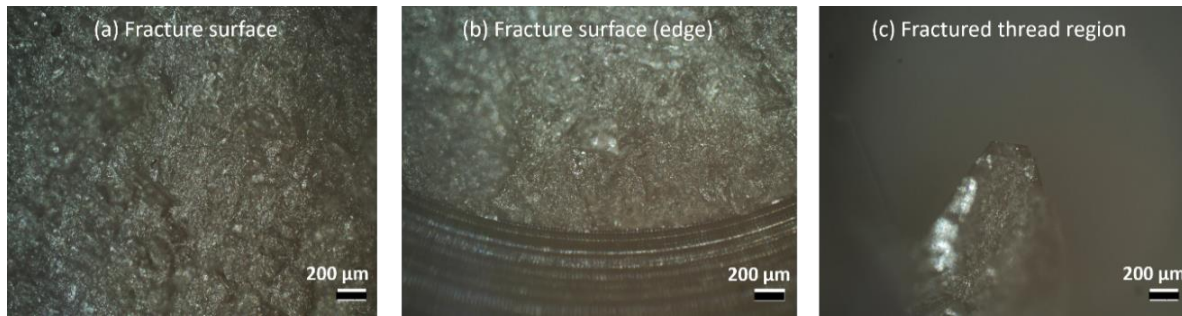


Figure 11: Optical micrographs of the fracture surface for the AM bolt with 2.5% porosity (S2.5) samples: (a) and (b) fracture surface; (c) location of fracture in the threaded region. Fracture occurred in the threaded region.

In contrast, the optical images for bolts with premature failure (Figure 12) show very different behavior, as expected. The transition between the primary and secondary crack is visible in Figures 12a-b, a feature observed in all bolts that cracked during the machining process. This crack transition propagated to the bottom surface of the bolt head, where it is visible as an external crack in Figure 12c. The images also reveal higher porosity and material inconsistency as compared to the images seen in Figures 10 and 11 above.

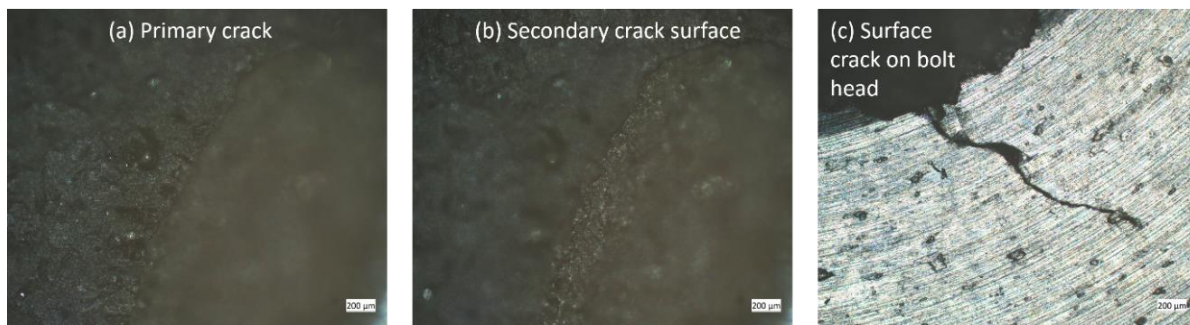


Figure 12: Fracture of S2.5 sample specimen with machining-induced crack showing (a) primary crack; (b) secondary crack; and (c) propagated cracked bolt head surface.

5 Conclusions and Future Work

This study evaluated the feasibility of manufacturing Ti64 aerospace bolts with lattice infill designs using laser powder bed fusion (LPBF) to simulate disruptions in the supply chain, reducing access to the raw material. The designs featured internal gyroid lattices to simulate progression of weight (and material) reductions, simulating the supply-chain disruptions in the form of limited access to feedstock material. The results demonstrate that additive manufacturing (AM) enables measurable weight reduction (up to 4.26 %) while retaining moderate tensile strength among LPBF variants. However, the AM-produced bolts exhibited a 40.5 % reduction in ultimate tensile load compared to machined bar stock, highlighting the negative influence of process-induced defects, microstructural anisotropy, and post-processing challenges, and leaving room for further detailed analysis and process optimization. While AM offers promising avenues for lightweight, on-demand fastener production under limited access to material, this study underscores the necessity of process optimization (including any post-processing) and deeper material structure-property-processing understanding before qualification can be achieved.

Overall, while AM shows promise as a resilient process owing to the customizability and the design freedom it enables, more systematic research is still required to fully answer the research query posed in this paper. Key limitations of this work include the restricted sample size, the absence of fatigue performance data, and the impact of surface roughness and machining-induced defects on mechanical reliability. The presence of residual powder within lattice structures also reduced the achieved weight savings, suggesting the need for improved powder removal techniques. Future research experiments would include fatigue testing to evaluate long-term performance under cyclic loading and further process optimization aimed at minimizing porosity, residual stress, and surface defects. Additionally, detailed metallographic characterization will be carried out to understand the influence of microstructure on the part properties. Larger sample sizes will be necessary to enable statistically robust conclusions regarding repeatability and reliability. Additionally, the development of predictive models correlating standard tensile coupon tests with the mechanical behavior of complex, lattice-optimized parts could lead to facilitating the qualification of AM parts such as fasteners.

Acknowledgements

The authors gratefully acknowledge Julio Andres Hernandez from the Herrick Laboratories at Purdue University for conducting the X-ray computed tomography scans. Additive manufacturing was carried out by Edgar James Yother V in the MMRL (Manufacturing and Materials Research Labs), and tensile testing was performed in collaboration with Clayton M. Kibbey. Machining support was provided by the Bechtel Innovation Design Center. The authors also thank the Purdue School of Mechanical Engineering for infrastructure support.

References

- [1] McGregor, M., Patel, S., Zhang, K., Yu, A., Vlasea, M., and McLachlin, S., 2024, "A Manufacturability Evaluation of Complex Architectures by Laser Powder Bed Fusion Additive Manufacturing," *J Manuf Sci Eng*, 146(6). <https://doi.org/10.1115/1.4065315>.

- [2] Moridi, A., Demir, A. G., Caprio, L., Hart, A. J., Previtali, B., and Colosimo, B. M., 2019, "Deformation and Failure Mechanisms of Ti-6Al-4V as Built by Selective Laser Melting," *Materials Science and Engineering: A*, 768, p. 138456. <https://doi.org/10.1016/j.msea.2019.138456>.
- [3] Moon, S., Ma, R., Attardo, R., Tomonto, C., Nordin, M., Wheelock, P., Glavicic, M., Layman, M., Billo, R., and Luo, T., 2021, "Impact of Surface and Pore Characteristics on Fatigue Life of Laser Powder Bed Fusion Ti-6Al-4V Alloy Described by Neural Network Models," *Sci Rep*, 11(1), p. 20424. <https://doi.org/10.1038/s41598-021-99959-6>.
- [4] Anderson, L. S., Venter, A. M., Vrancken, B., Marais, D., Van Humbeeck, J., and Becker, T. H., 2018, "Investigating the Residual Stress Distribution in Selective Laser Melting Produced Ti-6Al-4V Using Neutron Diffraction," *Materials Research Proceedings 4*, Materials Research Forum LLC, pp. 73–78. <https://doi.org/10.21741/9781945291678-11>.
- [5] Alami, A. H., Ghani Olabi, A., Alashkar, A., Alasad, S., Aljaghoub, H., Rezk, H., and Abdelkareem, M. A., 2023, "Additive Manufacturing in the Aerospace and Automotive Industries: Recent Trends and Role in Achieving Sustainable Development Goals," *Ain Shams Engineering Journal*, 14(11). <https://doi.org/10.1016/j.asej.2023.102516>.
- [6] Khan, N., and Riccio, A., 2024, "A Systematic Review of Design for Additive Manufacturing of Aerospace Lattice Structures: Current Trends and Future Directions," *Progress in Aerospace Sciences*, 149. <https://doi.org/10.1016/j.paerosci.2024.101021>.
- [7] Lopez, C., and Stroobants, J., 2019, "Lattice Topology Optimization and 3D Printing of a 316L Control Arm," *Sim-AM 2019: II International Conference on Simulation for Additive Manufacturing.*, pp. 186–192.
- [8] Palomino, D., McClelland, R., Grau, M., Watkins, R., and Li, B., 2023, "Design for Internal Lattice Structures with Application in Additive Manufacturing," *2023 International Solid Freeform Fabrication Symposium*, University of Texas at Austin. <https://doi.org/https://doi.org/10.26153/tsw/51081>.